

Fig. 1. Enzymatic reaction of the glycine cleavage system (GCS). One molecule of glycine is broken down, generating one molecule of carbon dioxide, ammonia, and one carbon unit. Note that ¹³CO₂ is synthesized from [1-¹³C]glycine.

AMT, *GCSH* and *DLG*. Dihydrolipoamide dehydrogenase is a so-called housekeeping enzyme that serves as a component of other complex enzyme systems such as the pyruvate dehydrogenase complex and the branched chain ketoacid dehydrogenase complex. No participation of other GCS components to other enzyme system has been reported to date.

Diagnosis of GE should be considered when neonates or infants develop seizures, muscular hypotonia, and lethargy that are not readily explicable on the basis of infection, trauma, hypoxia, or other commonly encountered pediatric problems. Differential diagnosis between GE and other diseases with hyperglycinemia is sometimes difficult. The absence of ketoacidosis is indicated by plasma bicarbonate levels and/or blood pH. Exclusion of organic acidemia by gas chromatographic analysis of urine or plasma are crucial [10]. In GE the glycine level in cerebrospinal fluids (CSF) is elevated and the ratio of CSF to plasma glycine concentration is increased more than 0.09, while in normal and ketotic hyperglycinemia it is below 0.04. An EEG finding of a burst suppression pattern is characteristic to GE in the first month of life.

As the clinical picture of GE is so highly heterogeneous, it may sometimes be difficult to diagnose GE solely on the basis of clinical symptoms and the amino acid analysis of CSF and serum. Atypical GE patients can have some residual GCS activities, as demonstrated by enzymatic analysis of GCS activity in liver samples [11] and by *in vitro* expression analysis of the identified mutations [6,12]. The elevations of glycine concentrations and the CSF/plasma glycine ratio in atypical GE are milder than those in typical cases. Furthermore, increased glycine levels and ratio have also been observed in other pathological conditions or as a result of technical artifacts or administration of certain drugs [10]. Therefore, the clinical diagnosis requires confirmation either by enzymatic analysis of the GCS in liver tissues obtained by invasive biopsy or the exhaustive mutational analysis of three responsible genes, *GLDC*, *AMT*, and *GCSH*. Both procedures are laborious, and require technical expertise, and are currently performed in only a limited number of laboratories.

Here we report a recent advance in diagnosis of GE by introducing two novel diagnostic methods, the ¹³C-glycine breath test and the multiplex ligation dependent

probe amplification (MLPA) method for detection for large deletions in *GLDC*. Both methods would facilitate confirmation of diagnosis of GE in patients with hyperglycinemia.

2. ¹³C-glycine breath test facilitating enzymatic diagnosis of GE

2.1. Principle of the ¹³C-glycine breath test

The activity of the GCS is currently measured *in vitro* by measuring the radioactivity of ¹⁴CO₂ generated from substrate, [1-¹⁴C]glycine [11]. When glycine is administered to normal subjects, it is decarboxylated predominantly by the GCS in liver, leading to production of CO₂. The amount of CO₂ production may be easily quantified if glycine is labeled with stable isotope, [1-¹³C]glycine. ¹³C is not radioactive, and can be safely administered to patients including children [13]. Since the generated ¹³CO₂ is excreted into exhaled breath one can evaluate the GCS activity *in vivo* by gathering exhaled breath for measurement of concentration of ¹³CO₂ [14].

2.2. Method of [1-¹³C]glycine breath test

The procedure of [1-¹³C]glycine breath test is shown in Fig. 2. [1-¹³C]glycine with >99% purity is used for the breath test. The ¹³C-glycine is administered orally at a dose of 10 mg/kg, a maximum dose of 100 mg. In the case that a subject is an infant or small child or a mentally-retarded child it is administered through gastric tubes. Before the administration of ¹³C-glycine, a reference breath sample was collected by using a face-mask equipped with a one-way air valve followed by transfer to the sampling bags. Test samples of 150–250 ml were collected from each subject at 15, 30, 45, 60, 90, 120, 180, 240, and 300 min after the administration of ¹³C-glycine. The difference of ¹³CO₂ concentration ($\Delta^{13}\text{CO}_2$) between reference and test breath samples was measured using an infrared ¹³CO₂ analyzer, UBit-IR300 (Otsuka Electronics, Osaka, Japan) [15]. Cumulative %recovery was calculated from administered dose (mg) of ¹³C-glycine, $\Delta^{13}\text{CO}_2$ values (%), body weight (kg), and body length (cm) as described [14].

2.3. Reliability of the ¹³C-glycine breath test

The breath test was performed in a total of 10 control subjects: 24.1 ± 4.0% of ¹³C was recovered within 5 h after administration of ¹³C-glycine. The ¹³C-glycine breath test was previously performed in neonates for evaluation of gastric emptying time [16]. The cumulative ¹³C recovery at 300 min after ¹³C-glycine administration was 21.5 ± 4.3% in healthy neonates, similar to that in our study. We therefore used 24.1 ± 4.0% as the

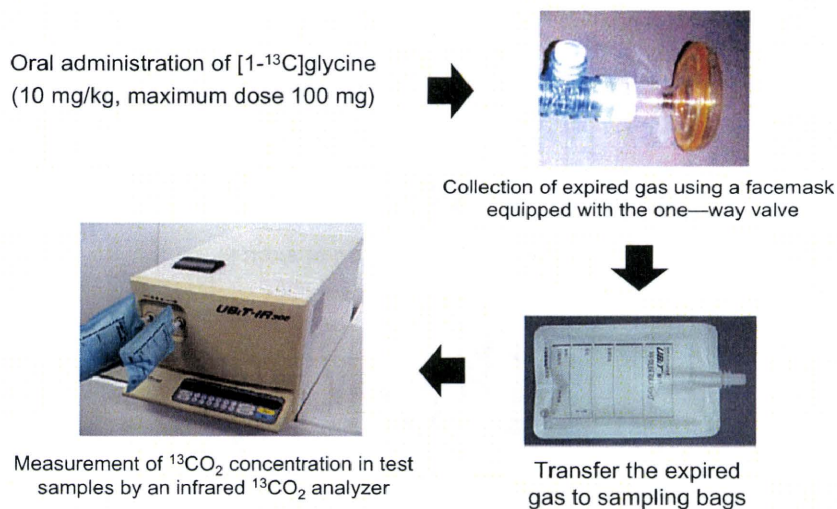


Fig. 2. Procedure of the ¹³C-glycine breath test. After the oral administration of [1-¹³C]glycine, expired gas of a subjects is collected with the facemask at each time point, which are subjected to measurement of ¹³CO₂ level by the infrared ¹³CO₂ analyzer.

control value. The breath test was then performed in five patients with GE. Their mean cumulative recovery was $8.3 \pm 2.3\%$, which was significantly lower than that in control subjects ($p < 0.0001$). Therefore, patients with GE could be readily distinguished from non-GE individuals. In contrast, the mean cumulative recovery in seven obligate carriers, the parents of the patients, was $22.9 \pm 3.3\%$, which is not significantly different from the control subjects, suggesting that carrier detection is extremely difficult. Patients with organic acidemia such as methylmalonic acidemia (MMA) or propionic acidemia are known to show secondary hyperglycinemia. A patient with MMA showed 18.1% cumulative recovery, which was slightly lower than the control mean by 1.3 SD. The GCS activity in liver specimens was reported in three patients with organic acidemia [17]. One patient on a low-protein diet had normal GCS activity in his biopsied liver sample. Two other patients who died with severe metabolic acidosis had markedly low GCS activities in their autopsied liver, suggesting that the hepatic GCS activity in patients with organic acidemia may be influenced by their metabolic status. Since the ¹³C-glycine breath test reflects the in vivo GCS activity, its result in patients with organic acidemia may fluctuate depending on their condition at the time of the test.

2.4. Utility of the ¹³C-glycine breath test

The ¹³C-glycine breath test is an in vivo assay of the GCS activity, which enables the rapid and reliable diagnosis of GE. The ¹³C-glycine breath test can be easily performed in neonates, small children and adult patients. The ¹³C-glycine stable isotope is not toxic. It has the advantages of being simple, non-invasive and widely available. Recently, a simple and inexpensive

¹³CO₂ analyzer using infrared spectrophotometry has been developed for the diagnosis of *Helicobacter pylori* infection by the ¹³C-urea test [18]. Since the infrared ¹³CO₂ analyzer is now widely distributed, the ¹³C-glycine breath could be readily accomplished in many hospitals and clinics. Diagnosis of atypical GE cases is often difficult by amino acid analysis alone as the CSF/plasma glycine ratio is not as high in atypical cases [4]. Since the assay conditions for measuring GCS activity differ in detail from laboratory to laboratory, it is difficult to compare the results from different laboratories. In contrast, the protocol for the ¹³C-breath test is readily standardized. It could become a standard test for the evaluation of the GCS activity, and facilitate early diagnosis of atypical GE.

3. MLPA analysis facilitating genetic diagnosis of GE

3.1. Mutations in the GCS genes

The GCS has three specific components encoded by *GLDC*, *AMT*, and *GCSH*. A comprehensive screening was performed for *GLDC*, *AMT*, and *GCSH* mutations in 56 patients with neonatal GE [19]. The *GLDC* mutations were identified in 36 of 56 (64%) patients while the *AMT* mutations were found in 6 of 56 patients (11%). No mutation was identified in *GCSH*. Both *GLDC* and *AMT* mutations were highly heterogeneous, including many private mutations. To our best knowledge, there are only two prevalent mutations, p.S564I in Fins [20] and p.R515S in Caucasians [21]. In 16 of the 36 (44%) patients with the *GLDC* mutations, mutations could be identified in only one allele despite extensive sequencing of the entire coding regions, suggesting that there are *GLDC* mutations that cannot be detected by the exon-sequencing method.

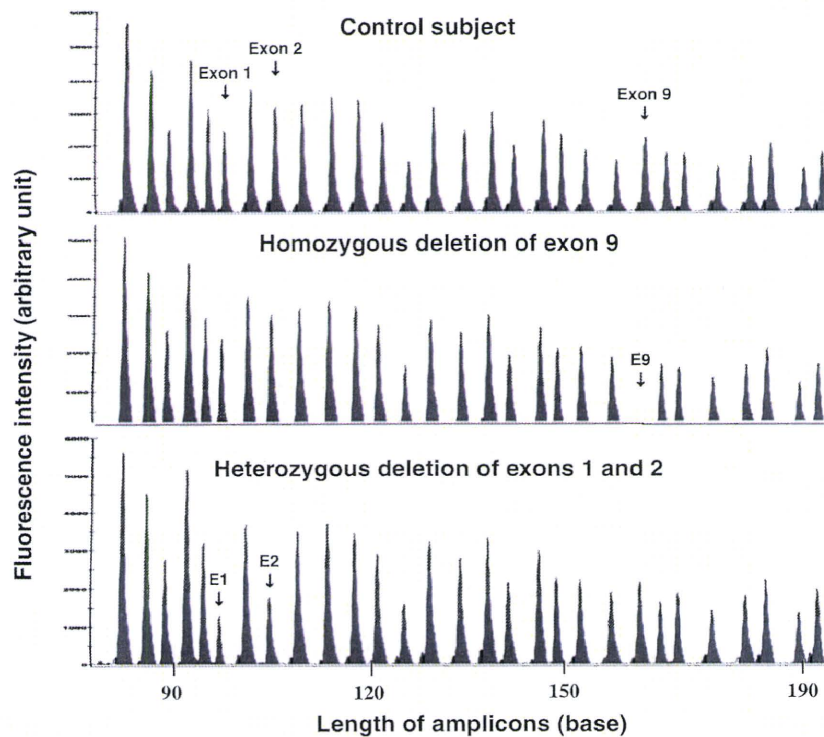


Fig. 3. Chromatogram of the multiplex ligation-dependent probe amplification (MLPA) analysis of a control subject and two GE patients. The horizontal axis indicates length of the PCR product and the vertical axis represents fluorescence intensity of each DNA fragment. A DNA fragment corresponding to *GLDC* exon 9 in a control subject (panel A) is completely missing in a GE patient with homozygous deletion of *GLDC* exon 9 (panel B). The peak areas of exons 1 and 2 are reduced in a GE patient with heterozygous deletion of *GLDC* exons 1 and 2 (panel C), compared with those in a control subject (panel A).

3.2. Detection of large deletion in *GLDC* by MLPA method

We previously encountered several patients with deletion of *GLDC* exon 1 [22]. Sellner et al. have reported a patient with deletion of the *GLDC* exons 2–15 [23]. Those observations suggested that a considerable number of *GLDC* deletions may remain unidentified. We have developed a screening system for deletions in *GLDC* by the MLPA method [24]. The MLPA method uses a pair of oligonucleotide probes, upstream and downstream probes, for each *GLDC* exon. The upstream probe is designed to locate in adjacent to the downstream probes. After hybridization of the oligonucleotide probes with the genomic DNA the hybridization mixtures are subject to ligation reaction. The upstream and downstream probes can be ligated only when they are hybridized with their target sequences. Both upstream and downstream probes have binding sequence for the universal PCR primers, which enables us to amplify the ligated probes by PCR with the universal primers. Allele number of each target exon can be evaluated by measuring amount of PCR products amplified from each ligated probes.

3.3. Screening of *GLDC* deletions in GE patients

Two distinct cohorts of patients with typical GE were screened by this MLPA method [24]: the first cohort consisted of 45 families with no identified *AMT* or *GCSH* mutations. The second cohort was comprised of 20 patients from the UK who were not prescreened for *AMT* mutations. Deletions in *GLDC* were identified in 16 of 90 alleles (18%) in the first cohort and 9 of 40 alleles (22.5%) in the second cohort. A total of 14 deletions with various lengths were identified, varying from a single exon to entire *GLDC* gene. Typical result of the MLPA analysis in the GE patients is shown in Fig. 3. Sequencing analysis of the flanking sequences of several deletions suggested that *Alu*-mediated recombination may underlie in the etiology of the *GLDC* deletions.

3.4. Utility of the MLPA test

Mutations in the GCS genes are highly heterogeneous in GE, suggesting necessity of sequencing entire coding regions of the GCS genes for genetic confirmation of GE. Full sequencing of three GCS genes is, however, too lengthy to perform for the clinical genetic testing

of GE. The *GLDC* deletions can be detected in more than 20% of GE mutant alleles in multiple ethnic groups, suggesting that the MLPA method is a good first line screening for the genetic testing of GE.

4. Conclusions

We described two laboratory tests, which have recently developed for the diagnosis of GE. Because both the [$1-^{13}\text{C}$]glycine breath test and the MLPA analysis are simple and efficient they would facilitate the confirming diagnosis of hyperglycinemic patients as having GE.

Acknowledgments

We are grateful to the families who participated in this study. This work was supported by a grant from the Ministry of Education, Culture, Sports, Science, and Technology in Japan, and a grant from the Ministry of Health, Labor, and Public Welfare in Japan.

This paper was presented in the Joint Meeting of Infantile Seizure Society (13th Annual Meeting) and Taiwan Child Neurology Society (14th Annual Meeting), International Symposium on Epilepsy in Neuro-metabolic Diseases, Taipei, Taiwan, March 26–28, 2010.

References

- [1] Tada K, Narisawa K, Yoshida T, Konno T, Yokoyama Y. Hyperglycinemia: a defect in glycine cleavage reaction. *Tohoku J Exp Med* 1969;98:289–96.
- [2] Hamosh A, Johnston MV. Nonketotic hyperglycinemia. In: Scriver C, Beaudet A, Sly W, Valle D, editors. *The metabolic and molecular bases of inherited disease*. New York: McGraw-Hill; 2001. p. 2065–78.
- [3] Hoover-Fong JE, Shah S, Van Hove JL, Applegarth D, Toone J, Hamosh A. Natural history of nonketotic hyperglycinemia in 65 patients. *Neurology* 2004;63:1847–53.
- [4] Christodoulou J, Kure S, Hayasaka K, Clarke JT. Atypical nonketotic hyperglycinemia confirmed by assay of the glycine cleavage system in lymphoblasts. *J Pediatr* 1993;123:100–2.
- [5] Flusser H, Korman SH, Sato K, Matsubara Y, Galil A, Kure S. Mild glycine encephalopathy (NKH) in a large kindred due to a silent exonic *GLDC* splice mutation. *Neurology* 2005;64:1426–30.
- [6] Dinopoulos A, Kure S, Chuck G, Sato K, Gilbert DL, Matsubara Y, et al. Glycine decarboxylase mutations: a distinctive phenotype of nonketotic hyperglycinemia in adults. *Neurology* 2005;64:1255–7.
- [7] Percy A. Nonketotic hyperglycinemia in adults: anticipating the unexpected. *Neurology* 2005;64:1105.
- [8] Kikuchi G. The glycine cleavage system: composition, reaction mechanism, and physiological significance. *Mol Cell Biochem* 1973;1:169–87.
- [9] Sakata Y, Owada Y, Sato K, Kojima K, Hisanaga K, Shinka T, et al. Structure and expression of the glycine cleavage system in rat central nervous system. *Brain Res Mol Brain Res* 2001;94:119–30.
- [10] Korman SH, Gutman A. Pitfalls in the diagnosis of glycine encephalopathy (non-ketotic hyperglycinemia). *Dev Med Child Neurol* 2002;44:712–20.
- [11] Hayasaka K, Tada K, Fueki N, Nakamura Y, Nyhan WL, Schmidt K, et al. Nonketotic hyperglycinemia: analyses of glycine cleavage system in typical and atypical cases. *J Pediatr* 1987;110:873–7.
- [12] Kure S, Ichinohe A, Kojima K, Sato K, Kizaki Z, Inoue F, et al. Mild variant of nonketotic hyperglycinemia with typical neonatal presentations: mutational and in vitro expression analyses in two patients. *J Pediatr* 2004;144:827–9.
- [13] Ohara H, Suzuki T, Nakagawa T, Yoneshima M, Yamamoto M, Tsujino D, et al. ^{13}C -UBT using an infrared spectrometer for detection of *Helicobacter pylori* and for monitoring the effects of lansoprazole. *J Clin Gastroenterol* 1995;20:S115–7.
- [14] Kure S, Korman SH, Kanno J, Narisawa A, Kubota M, Takayanagi T, et al. Rapid diagnosis of glycine encephalopathy by ^{13}C -glycine breath test. *Ann Neurol* 2006;59:862–7.
- [15] Kure S, Sato K, Fujii K, Aoki Y, Suzuki Y, Kato S, et al. Wild-type phenylalanine hydroxylase activity is enhanced by tetrahydrobiopterin supplementation in vivo: an implication for therapeutic basis of tetrahydrobiopterin-responsive phenylalanine hydroxylase deficiency. *Mol Genet Metab* 2004;83:150–6.
- [16] Oishi M, Nishida H, Hoshi J. ^{13}C -glycine breath test to measure gastric emptying of neonates (in Japanese). ^{13}C Igaku 1996;7:32–3.
- [17] Hayasaka K, Narisawa K, Satoh T, Tateda H, Metoki K, Tada K, et al. Glycine cleavage system in ketotic hyperglycinemia: a reduction of H-protein activity. *Pediatr Res* 1982;16:5–7.
- [18] Ohara H, Suzuki T, Nakagawa T, Yoneshima M, Yamamoto M, Tsujino D, et al. ^{13}C -UBT using an infrared spectrometer for detection of *Helicobacter pylori* and for monitoring the effects of lansoprazole. *J Clin Gastroenterol* 1995;20:S115–7.
- [19] Kure S, Kato K, Dinopoulos A, Gail C, DeGrauw TJ, Christodoulou J, et al. Comprehensive mutation analysis of *GLDC*, *AMT*, and *GCSH* in nonketotic hyperglycinemia. *Hum Mutat* 2006;27:343–52.
- [20] Kure S, Takayanagi M, Narisawa K, Tada K, Leisti J. Identification of a common mutation in Finnish patients with nonketotic hyperglycinemia. *J Clin Invest* 1992;90:160–4.
- [21] Toone JR, Applegarth DA, Coulter-Mackie MB, James ER. Recurrent mutations in P- and T-proteins of the glycine cleavage complex and a novel T-protein mutation (N145I): a strategy for the molecular investigation of patients with nonketotic hyperglycinemia (NKH). *Mol Genet Metab* 2001;72:322–5.
- [22] Takayanagi M, Kure S, Sakata Y, Kurihara Y, Ohya Y, Kajita M, et al. Human glycine decarboxylase gene (*GLDC*) and its highly conserved processed pseudogene (*psiGLDC*): their structure and expression, and the identification of a large deletion in a family with nonketotic hyperglycinemia. *Hum Genet* 2000;106:298–305.
- [23] Sellner L, Edkins E, Greed L, Lewis B. Detection of mutations in the glycine decarboxylase gene in patients with nonketotic hyperglycinaemia. *Mol Genet Metab* 2005;84:167–71.
- [24] Kanno J, Hutchin T, Kamada F, Narisawa A, Aoki Y, Matsubara Y, et al. *J Med Genet* 2007;44:e69.

ORIGINAL ARTICLE

A genome-wide association study identifies *RNF213* as the first Moyamoya disease gene

Fumiaki Kamada¹, Yoko Aoki¹, Ayumi Narisawa^{1,2}, Yu Abe¹, Shoko Komatsuzaki¹, Atsuo Kikuchi³, Junko Kanno¹, Tetsuya Niihori¹, Masao Ono⁴, Naoto Ishii⁵, Yuji Owada⁶, Miki Fujimura², Yoichi Mashimo⁷, Yoichi Suzuki⁷, Akira Hata⁷, Shigeru Tsuchiya³, Teiji Tominaga², Yoichi Matsubara¹ and Shigeo Kure^{1,3}

Moyamoya disease (MMD) shows progressive cerebral angiopathy characterized by bilateral internal carotid artery stenosis and abnormal collateral vessels. Although ~15% of MMD cases are familial, the MMD gene(s) remain unknown. A genome-wide association study of 785 720 single-nucleotide polymorphisms (SNPs) was performed, comparing 72 Japanese MMD patients with 45 Japanese controls and resulting in a strong association of chromosome 17q25-ter with MMD risk. This result was further confirmed by a locus-specific association study using 335 SNPs in the 17q25-ter region. A single haplotype consisting of seven SNPs at the *RNF213* locus was tightly associated with MMD ($P=5.3 \times 10^{-10}$). *RNF213* encodes a really interesting new gene finger protein with an AAA ATPase domain and is abundantly expressed in spleen and leukocytes. An RNA *in situ* hybridization analysis of mouse tissues indicated that mature lymphocytes express higher levels of *Rnf213* mRNA than their immature counterparts. Mutational analysis of *RNF213* revealed a founder mutation, p.R4859K, in 95% of MMD families, 73% of non-familial MMD cases and 1.4% of controls; this mutation greatly increases the risk of MMD ($P=1.2 \times 10^{-43}$, odds ratio=190.8, 95% confidence interval=71.7–507.9). Three additional missense mutations were identified in the p.R4859K-negative patients. These results indicate that *RNF213* is the first identified susceptibility gene for MMD.

Journal of Human Genetics (2011) 56, 34–40; doi:10.1038/jhg.2010.132; published online 4 November 2010

INTRODUCTION

'Moyamoya' is a Japanese expression for something hazy, such as a puff of cigarette smoke drifting in the air. In individuals with Moyamoya disease (MMD), there is a progressive stenosis of the internal carotid arteries; a fine network of collateral vessels, which resembles a puff of smoke on a cerebral angiogram, develops at the base of the brain (Figure 1a).^{1,2} This steno-occlusive change can cause transient ischemic attacks and/or cerebral infarction, and rupture of the collateral vessels can cause intracranial hemorrhage. Children under 10 years of age account for nearly 50% of all MMD cases.³

The etiology of MMD remains unclear, although epidemiological studies suggest that bacterial or viral infection may be implicated in the development of the disease.⁴ Growing attention has been paid to the upregulation of arteriogenesis and angiogenesis associated with MMD because chronic ischemia in other disease conditions is not always associated with a massive development of collateral vessels.^{5,6} Several angiogenic growth factors are thought to have functions in the development of MMD.⁷

Several lines of evidence support the importance of genetic factors in susceptibility to MMD.⁸ First, 10–15% of individuals with MMD

have a family history of the disease.⁹ Second, the concordance rate of MMD in monozygotic twins is as high as 80%.¹⁰ Third, the prevalence of MMD is 10 times higher in East Asia, especially in Japan (6 per 100 000 population), than in Western countries.³ Familial MMD may be inherited in an autosomal dominant fashion with low penetrance or in a polygenic manner.¹¹ Linkage studies of MMD families have revealed five candidate loci for an MMD gene: chromosomes 3p24–26,¹² 6q25,¹³ 8q13–24,¹⁰ 12p12–13¹⁰ and 17q25.¹⁴ However, no susceptibility gene for MMD has been identified to date.

We collected 20 familial cases of MMD to investigate linkage in the five putative MMD loci. However, a definitive result was not obtained for any of the loci. We then hypothesized that there might be a founder mutation among Japanese patients with MMD because the prevalence of MMD is unusually high in Japan.¹⁵ Genome-wide and locus-specific association studies were performed and successfully identified a single gene, *RNF213*, linked to MMD. We report here a strong association between MMD onset and a founder mutation in *RNF213*, as well as the expression profiles of *RNF213*, in various tissues.

¹Department of Medical Genetics, Tohoku University School of Medicine, Sendai, Japan; ²Department of Neurosurgery, Tohoku University School of Medicine, Sendai, Japan; ³Department of Pediatrics, Tohoku University School of Medicine, Sendai, Japan; ⁴Department of Pathology, Tohoku University School of Medicine, Sendai, Japan; ⁵Department of Microbiology and Immunology, Tohoku University School of Medicine, Sendai, Japan; ⁶Department of Organ Anatomy, Yamaguchi University Graduate School of Medicine, Ube, Japan and ⁷Department of Public Health, Graduate School of Medicine, Chiba University, Chiba, Japan

Correspondence: Dr S Kure, Department of Pediatrics, Tohoku University School of Medicine, 1-1 Seiry-machi, Aoba-ku, Miyagi, Sendai 980-8574, Japan.

E-mail: kure@med.tohoku.ac.jp

Received 30 September 2010; accepted 1 October 2010; published online 4 November 2010

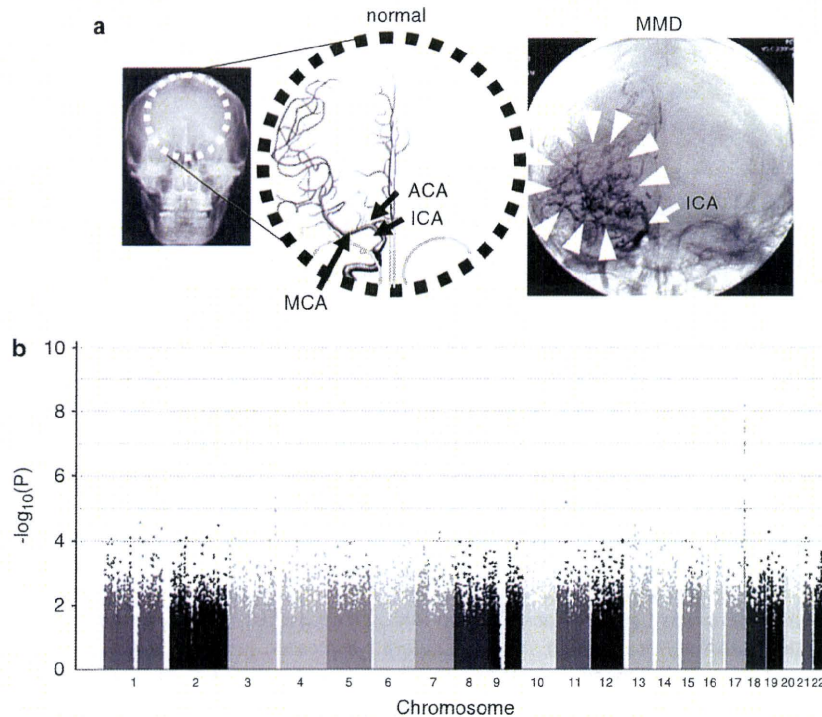


Figure 1 (a) Abnormal brain vessels in MMD. The dotted circle indicates the X-ray field of cerebral angiography (left panel). Normal structures of the right internal carotid artery (ICA), anterior cerebral artery (ACA) and middle cerebral artery (MCA) are illustrated (middle panel). The arrowheads indicate abnormal collateral vessels appearing like a puff of smoke in the angiogram of an individual with MMD (right panel). Note that ACA and MCA are barely visible, because of the occlusion of the terminal portion of the ICA. (b) Manhattan plot of the 785 720 SNPs used in the genome-wide association analysis of MMD patients. Note that the SNPs in the 17q25-ter region reach a significance of $P < 10^{-8}$.

MATERIALS AND METHODS

Affected individuals

Genomic DNA was extracted from blood and/or saliva samples obtained from members of the families with MMD (Supplementary Figure 1), MMD patients with no family history and control subjects. All of the subjects were Japanese. MMD was diagnosed on the basis of guidelines established by the Research Committee on Spontaneous Occlusion of the Circle of Willis of the Ministry of Health and Welfare of Japan. This study was approved by the Ethics Committee of Tohoku University School of Medicine. Total RNA samples were purified from leukocytes using an RNeasy mini kit (Qiagen, Hilden, Germany) and used as templates for cDNA synthesis with an Oligo (dT)₂₀ primer and SuperScript II reverse transcriptase according to the manufacturer's instructions (Invitrogen, Carlsbad, CA, USA).

Linkage analysis

For the linkage analysis, DNA samples were genotyped for 36 microsatellite markers within five previously reported MMD loci using the ABI 373A DNA Sequencer (Applied Biosystems, Foster City, CA, USA). Pedigrees and haplotypes were constructed with the Cyrillic version 2.1 software (Oxfordshire, UK). Multipoint analyses were conducted using the GENEHUNTER 2 software (<http://www.broadinstitute.org/ftp/distribution/software/genehunter/>). Statistical analysis was performed with SPSS version 14.0J (SPSS, Tokyo, Japan).

Genome-wide and locus-specific association studies

A genome-wide association study was performed using a group of 72 MMD patients, which consisted of 64 patients without a family history of MMD and 8 probands of MMD families. The Illumina Human Omni-Quad 1 chip (Illumina, San Diego, CA, USA) was used for genotyping, and single-nucleotide polymorphisms (SNPs) with a genotyping completion rate of 100% were used for further statistical analysis (785 720 out of 1 140 419 SNPs). Genotyping data

from 45 healthy Japanese controls were obtained from the database at the International HapMap Project web site. The 785 720 SNPs were statistically analyzed using the PLINK software (<http://pngu.mgh.harvard.edu/~purcell/plink/index.shtml>). For a locus-specific association study, we used 63 DNA samples consisting of 58 non-familial MMD patients and 5 probands of MMD families. A total of 384 SNPs within chromosome 17q25-ter were genotyped (Supplementary Table 1), using the GoldenGate Assay and a custom SNP chip (Illumina). Genotyping data for 45 healthy Japanese were used as a control. Case-control single-marker analysis, haplotype frequency estimation and significance testing of differences in haplotype frequency were performed using the Haploview version 3.32 program (<http://www.broad.mit.edu/mpg/haploview/>).

Mutation detection

Mutational analyses of *RNF213* and *FLJ35220* were performed by PCR amplification of each coding exon and putative promoter regions, followed by direct sequencing. Genomic sequence data for the two genes were obtained from the National Center for Biotechnology Information web site (<http://www.ncbi.nlm.nih.gov/>) for design of exon-specific PCR primers. *RNF213* cDNA fragments were amplified from leukocyte mRNA for sequencing analysis. Sequencing of the PCR products was performed with the ABI BigDye Terminator Cycle Sequencing Reaction Kit using the ABI 310 Genetic Analyzer. Identified base changes were screened in control subjects. Statistical difference of the carrier frequency of each base change was estimated by Fisher's exact test (the MMD group vs the control group).

Quantitative PCR

MTC Multiple Tissue cDNA Panels (Clontech Laboratory, Madison, WI, USA) were the source of cDNAs from human cell lines, adult and fetal tissues. Mononuclear cells and polymorphonuclear cells were isolated from the fresh peripheral blood of healthy human adults using Polymorphprep (Cosmo Bio,

Carlsbad, CA, USA). T and B cells were isolated from the fresh peripheral blood of healthy human adults using the autoMACS separator (Milteny Biotec, Bergisch Gladbach, Germany). Total RNA was isolated from these cells with the RNeasy Mini Kit (Qiagen) following the manufacturer's instructions. We reverse transcribed 100 ng samples of total RNA into cDNAs using the High Capacity cDNA Reverse Transcription Kit (Applied Biosystems). Quantitative PCRs were performed in a final volume of 20 µl using the FastStart TaqMan Probe Master (Roche) (Roche, Madison, WI, USA), 5 µl of cDNA, 10 µM of *RNF*- or *GAPDH*-specific primers and 10 µM of probes (Universal ProbeLibrary Probe #80 for *RNF213* and Roche Probe #60 for *GAPDH*). All reactions were performed in triplicate using the ABI 7500 Real-Time PCR system (Applied Biosystems). Cycling conditions were 2 min at 50°C and 10 min at 95°C, followed by 40 cycles of 15 s at 95°C and 60 s at 60°C. Real-time PCR data were analyzed by the SDS version 1.2.1 software (Applied Biosystems). We evaluated the relative level of *RNF213* mRNA by determining the C_T value, the PCR cycle at which the reporter fluorescence exceeded the signal baseline. *GAPDH* mRNA was used as an internal reference for normalization of the quantitative expression values.

Multiplex PCR

MTC Multiple Tissue cDNA Panels (Clontech) were the source of human cell lines and cDNAs from human adult and fetal tissues. Multiplex PCRs were performed in a final volume of 20 µl using the Multiplex PCR Master Mix (Qiagen), 2 µl of cDNA, a 2 µM concentration of *RNF213* and a 10 µM concentration of *GAPDH*-specific primers. The samples were separated on a 2% agarose gel stained with ethidium bromide. Cycling conditions were 15 min at 94°C, followed by 30 cycles of 30 s at 94°C, 30 s at 57°C and 30 s at 72°C. For normalization of the expression levels, we used *GAPDH* as an internal reference for each sample.

In situ hybridization (ISH) analysis

Paraffin-embedded blocks and sections of mouse tissues for ISH were obtained from Genostaff (Tokyo, Japan). The mouse tissues were dissected, fixed with Tissue Fixative (Genostaff), embedded in paraffin by proprietary procedures (Genostaff) and sectioned at 6 µm. To generate anti-sense and sense RNA probes, a 521-bp DNA fragment corresponding to nucleotide positions 470–990 of mouse *Rnf213* (BC038025) was subcloned into the pGEM-T Easy vector (Promega, Madison, WI, USA). Hybridization was performed with digoxigenin-labeled RNA probes at concentrations of 300 ng ml⁻¹ in Probe Diluent-1 (Genostaff) at 60°C for 16 h. Coloring reactions were performed with NBT/BCIP solution (Sigma-Aldrich, St Louis, MO, USA). The sections were counterstained with Kernechtrot stain solution (Mutoh, Tokyo, Japan), dehydrated and mounted with Malinol (Mutoh). For observation of *Rnf213* expression in activated lymphocytes, 10-week-old Balb/c mice were intraperitoneally injected with 100 µg of keyhole limpet hemocyanin and incomplete adjuvant and sacrificed in 2 weeks. The spleen of the mice was removed for Hematoxylin–eosin staining and ISH analyses.

RESULTS

Using 20 Japanese MMD families, we reevaluated the linkage mapped previously to five putative MMD loci. No locus with significant linkage, Lod score >3.0 or NPL score >4.0 was confirmed (Supplementary Figure 2). We conducted a genome-wide association study of 72 Japanese MMD cases. Single-marker allelic tests comparing the 72 MMD cases and 45 controls were performed for 785 720 SNPs using χ^2 statistics. These tests identified a single locus with a strong association with MMD ($P < 10^{-8}$) on chromosome 17q25-ter (Figure 1b), which is in line with the latest mapping data of a MMD locus.¹⁶ The SNP markers with $P < 10^{-6}$ are listed in Table 1. To confirm this observation, we performed a locus-specific association study. A total of 384 SNP markers (Supplementary Table 1) were selected within the chromosome 17q25-ter region and genotyped in a set of 63 MMD cases and 45 controls. The SNP markers demonstrating a high association with MMD ($P < 10^{-6}$) were clustered in a 151-kb region from base position 75 851 399–76 003 020 (SNP No.116–136 in

Table 1 A genome-wide association study of Japanese MMD patients and controls

1	SNP	Chromosome	Base position	Gene	Risk allele/non-risk allele		Risk allele frequency in MMD	Risk allele frequency in controls	χ^2	P-value	95% confidence interval	
					T/C	A/G					Lower	Upper
1	rs11870849	17	76 025 668	RNF213	T/C	0.4792	0.1111	33.55	6.95E-09	7.36	3.532	15.34
2	rs6565681	17	75 963 089	RNF213	A/G	0.7361	0.3667	31.35	2.16E-08	4.819	2.733	8.489
3	rs7216493	17	75 941 953	RNF213	G/A	0.75	0.3889	30.39	3.53E-08	4.715	2.673	8.313
4	rs7217421	17	75 850 055	RNF213	A/G	0.6667	0.3	29.86	4.64E-08	4.666	2.642	8.237
5	rs12449863	17	75 857 806	RNF213	C/T	0.6667	0.3	29.86	4.64E-08	4.666	2.642	8.237
6	rs4890009	17	75 926 103	RNF213	G/A	0.8819	0.5778	28.5	9.38E-08	5.459	2.831	10.527
7	SNP17-75933731	17	75 933 731	RNF213	G/A	0.8819	0.5778	28.5	9.38E-08	5.458	2.831	10.527
8	rs7219131	17	75 867 365	RNF213	T/C	0.6667	0.3111	28.11	1.15E-07	4.429	2.517	7.794
9	rs6565677	17	75 932 037	RNF213	T/C	0.7431	0.3977	27.43	1.63E-07	4.378	2.483	7.722
10	rs4889848	17	75 969 256	RNF213	C/T	0.75	0.4111	26.99	2.05E-07	4.297	2.444	7.889
11	rs7224239	17	75 969 771	RNF213	A/G	0.8681	0.5667	26.99	2.05E-07	5.03	2.659	9.529

Abbreviations: MMD, moyamoya disease; SNP, single-nucleotide polymorphism. A genome-wide association study testing 1 140 419 SNPs on the Human Omni-Quad 1 chip (Illumina, San Diego, CA, USA) was performed in 72 Japanese MMD cases. Single-marker allelic tests between the cases and controls were performed using χ^2 statistics for all markers. This table lists the 11 SNP markers with a significance of $P < 10^{-6}$.

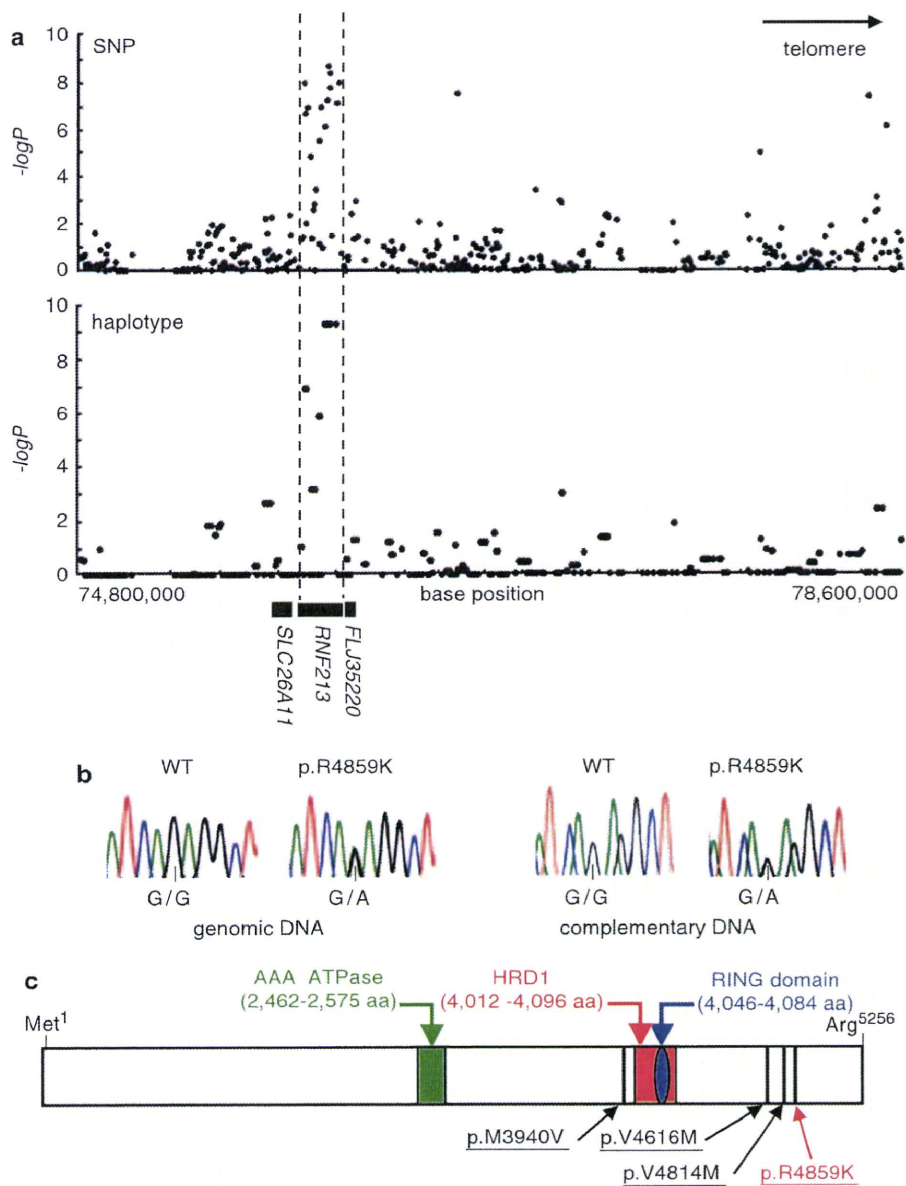


Figure 2 (a) Association analysis of 63 non-familial MMD cases and 45 control subjects. Statistical significance was evaluated by the χ^2 -test. SNP markers with a strong association with MMD ($P < 10^{-6}$) clustered in a 161-kb region (base position 75 851 399–76 012 838) indicated by two dotted lines (upper panel), which included the entire region of *RNF213* (lower panel). Haplotype analysis revealed a strong association ($P = 5.3 \times 10^{-10}$) between MMD and a single haplotype located within *RNF213*. (b) Sequencing chromatograms of the identified MMD mutations. The left panel shows the sequences of an unaffected individual and a carrier of a p.R4859K heterozygous mutation. Note that both wild-type and mutant alleles were expressed in leukocytes. (c) The structure of the RNF213 protein. The RNF213 protein contains three characteristic structures, the AAA-superfamily ATPase motif, the RING motif and the HMG-CoA reductase degradation motif. The positions of four mutations identified in MMD patients are underlined, including one prevalent mutation (red) and three private mutations (black).

Supplementary Table 1); this entire region was within the *RNF213* locus (Figure 2a). A single haplotype determined by seven SNPs (SNP Nos.130–136 in Supplementary Table 1) that resided in the 3' region of *RNF213* was strongly associated with MMD onset ($P = 5.3 \times 10^{-10}$). Analysis of the linkage disequilibrium block indicated that this haplotype was not in complete linkage disequilibrium with any other haplotype in this region (Supplementary Figure 3). These results strongly suggest that a founder mutation may exist in the 3' part of *RNF213*.

Mutational analysis of the entire coding and promoter regions of *RNF213* and *FLJ35220*, a gene 3' adjacent to *RNF213*, revealed that 19 of the 20 MMD families shared the same single base substitution, c.14576G>A, in exon 60 of *RNF213* (Figure 2b and Table 2). This nucleotide change causes an amino-acid substitution from arginine⁴⁸⁵⁹ to lysine⁴⁸⁵⁹ (p.R4859K). The p.R4859K mutation was identified in 46 of 63 non-familial MMD cases (73%), including 45 heterozygotes and a single homozygote (Table 3). Both the wild-type and the p.R4859K mutant alleles were co-expressed in leukocytes

Table 2 Nucleotide changes with amino-acid substitutions identified in the sequencing analysis of *RNF213* and *FLJ35220*

Gene	Exon	Nucleotide change ^a (amino-acid substitution)	Genotype (allele)		P-value ^b	χ^2 (df=1) ^c	Odds ratio (95% CI)
			Non-familial cases	Control subjects			
<i>RNF213</i>	29	c.7809C>A (p.D2603E)	2/63 (2/126)	15/381 (15/762)	0.77	0.09	0.80 (0.2–3.6)
<i>RNF213</i>	41	c.11818A>G (p.M3940V)	1/63 (1/126)	0/388 (0/776)	0.01	6.17	ND
<i>RNF213</i>	41	c.11891A>G (p.E3964G)	4/63 (4/126)	3/55 (4/110)	0.84	0.04	1.2 (0.3–5.5)
<i>RNF213</i>	52	c.13342G>A (p.A4448T)	4/63 (4/126)	2/53 (2/106)	0.53	0.39	1.7 (0.3–9.8)
<i>RNF213</i>	56	c.13846G>A (p.V4616M)	1/63 (1/126)	0/388 (0/776)	0.01	6.17	ND
<i>RNF213</i>	59	c.14440G>A (p.V4814M)	1/63 (1/126)	0/388 (0/776)	0.01	6.17	ND
<i>RNF213</i>	60	c.14576G>A (p.R4859K)	46/63 (47/126)	6/429 (6/858)	1.2×10^{-43}	298.1	190.8 (71.7–507.9)
<i>FLJ35220</i>		None					

Abbreviations: ND, not determined; SNP, single-nucleotide polymorphism.

^aNucleotide numbers of *RNF213* cDNA are counted from the A of the ATG initiator methionine codon (NCBI Reference sequence, NP_065965.4).

^bP-values were calculated by Fisher's exact test.

^cGenotypic distribution (carrier of the polymorphism vs non-carrier).

Table 3 Association of the p.R4859K (c.14576G>A) mutation with MMD

	Total	Genotype		
		wt/wt (%)	wt/p.R4859K (%)	p.R4859K/p.R4859K (%) ^d
Members of 19 MMD families^a				
Affected	42	0	39 (92.9)	3 (7.1)
Not affected	28	15 (53.6)	13 (46.4)	0
Individuals without a family history of MMD^{b,c}				
Affected	63	17 (27.0)	45 (71.4)	1 (1.6)
Not affected	429	423 (98.6)	6 (1.4)	0

Abbreviations: MMD, moyamoya disease.

^aEntire distribution, $\chi^2=29.4$, $P=4.2 \times 10^{-7}$.

^bEntire distribution, $\chi^2=298.2$, $P=1.8 \times 10^{-65}$.

^cGenotypic distribution (p.R4859K carrier vs non-carrier), $\chi^2=298.1$, $P=1.2 \times 10^{-43}$, odds ratio=190.8 (95% CI=71.7–507.9).

^dThe age of onset and initial symptoms of the four homozygotes were comparable to those of the 84 heterozygous patients.

in three patients heterozygous for the p.R4859K mutation (Figure 2b), excluding the possible instability of the mutant *RNF213* mRNA. Additional missense mutations, p.M3940V, p.V4616M and p.V4814M, were detected in three non-familial MMD cases without the p.R4859K mutation (Figure 2c). These mutations were not found in 388 control subjects and were detected in only one patient, suggesting that they were private mutations (Table 2). No copy number variation or mutation was identified in the *RNF213* locus of 12 MMD patients using comparative genome hybridization microarray analysis (Supplementary Figure 4). In total, 6 of the 429 control subjects (1.4%) were found to be heterozygous carriers of p.R4859K. Therefore, we concluded that the p.R4859K mutation increases the risk of MMD by a remarkably high amount (odds ratio=190.8 (95% confidence interval=71.7–507.9), $P=1.2 \times 10^{-43}$) (Table 3). It was recently reported that an SNP (ss161110142) in the promoter region of *RPTOR*, which is located ~150 kb downstream from *RNF213*, was associated with MMD.¹⁷ Genotyping of the SNP in *RPTOR* showed that the *RNF213* p.R4859K mutation was more strongly associated with MMD than ss161110142 (Supplementary Figure 1).

RNF213 encodes a protein with 5256 amino acids harboring a RING (really interesting new gene) finger motif, suggesting that it

functions as an E3 ubiquitin ligase (Figure 2c). It also has an AAA ATPase domain, which is characteristic of energy-dependent unfoldases.¹⁸ To our knowledge, *RNF213* is the first RING finger protein known to contain an AAA ATPase domain. The expression profile of *RNF213* has not been previously fully characterized. We performed a quantitative reverse transcription PCR analysis in various human tissues and cells. *RNF213* mRNA was highly expressed in immune tissues, such as spleen and leukocytes (Figure 3a and Supplementary Figure 5). Expression of *RNF213* was detected in fractions of both polymorphonuclear cells and mononuclear cells and was found in both B and T cell fractions (Supplementary Figure 6). A low but significant expression of *RNF213* was also observed in human umbilical vein endothelial cells and human pulmonary artery smooth muscle cells. Cellular expression was not enhanced in tumor cell lines, compared with leukocytes. In human fetal tissues, the highest expression was observed in leukocytes and the thymus (Supplementary Figure 6E). The expression of *RNF213* was surprisingly low in both adult and fetal brains. Overall, *RNF213* was ubiquitously expressed, and the highest expression was observed in immune tissues.

We studied the cellular expression of *Rnf213* in mice. The ISH analysis of spleen showed that *Rnf213* mRNA was present in small mononuclear cells, which were mainly localized in the white pulps (Figures 3b–g). The ISH signals were also detected in the primary follicles in the lymph node and in thymocytes in the medulla of the thymus (Supplementary Figure 7). To study *Rnf213* expression in activated lymphocytes we immunized mice with keyhole limpet hemocyanin, and examined *Rnf213* mRNA in spleen by ISH analysis. Primary immunization with keyhole limpet hemocyanin antigen revealed that the expression of *Rnf213* in the secondary follicle is as high as in the primary follicle in the lymph node (Supplementary Figure 8). In an E16.5 mouse embryo, expression was observed in the medulla of the thymus and in the cells around the mucous palatine glands (Supplementary Figure 9). These findings suggest that mature lymphocytes in a static state express *Rnf213* mRNA at a higher level than do their immature counterparts.

DISCUSSION

We identified a susceptibility locus for MMD by genome-wide and locus-specific association studies. Further sequencing analysis revealed a founder missense mutation in *RNF213*, p.R4859K, which was tightly associated with MMD onset. Identification of a founder mutation in individuals with MMD would resolve the following recurrent

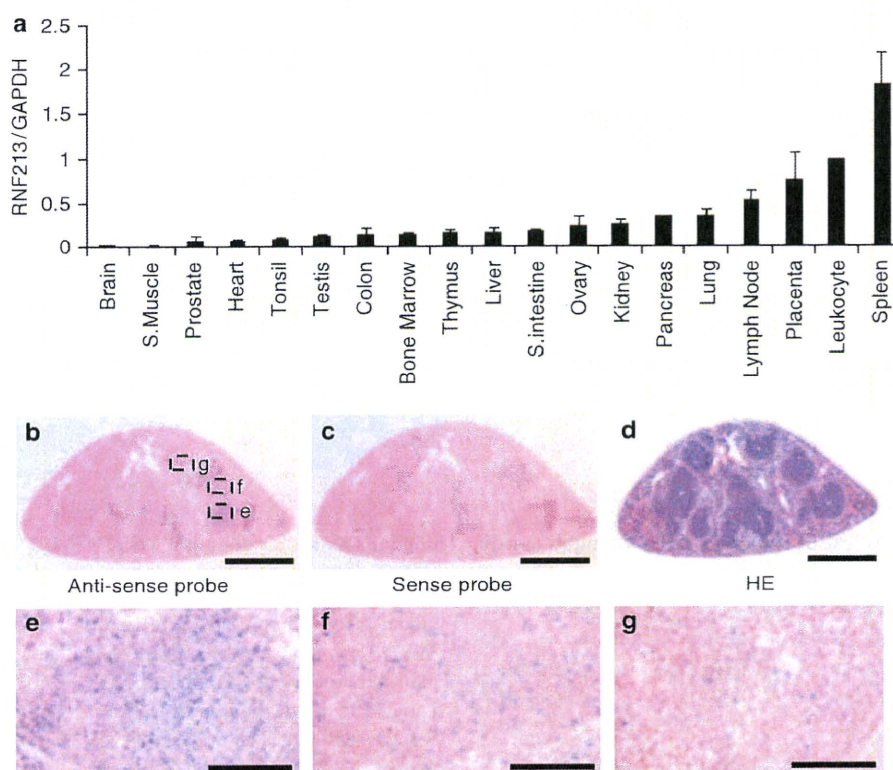


Figure 3 Expression of human *RNF213* and murine *Rnf213*. (a) RT-PCR analysis of *RNF213* mRNA in various human tissues. The expression levels of *RNF213* mRNA in various adult human tissues were evaluated by quantitative PCR using *GAPDH* mRNA as a control. The signal ratio of *RNF213* mRNA to *GAPDH* mRNA in each sample is shown on the vertical axis. (b–g) *In situ* hybridization (ISH) analysis of *Rnf213* mRNA in mouse spleen. Specific signals for *Rnf213* mRNA were detected by ISH analysis with the anti-sense probe (b) but not with the sense probe (c). Hematoxylin–eosin staining of the mouse spleen (d). Signals for the *Rnf213* mRNA were observed in small mononuclear cells, which were mainly localized in the white pulps (dotted square, e) and partially distributed in the red pulps (dotted squares, f and g). Panels e, f and g show the high-magnification images of the corresponding fields in panel b. Scale bars, 1 mm (b–d) and 50 μ m (e–g).

questions:^{2,19} (i) why is MMD more prevalent in East Asia than in Western countries? The carrier frequency of p.R4859K in Japan is 1/72 (Table 2). In contrast, we found no p.R4859K carrier in 400 Caucasian controls (data not shown). Furthermore, no mutation was identified in five Caucasian patients with MMD after the full sequencing of *RNF213*. These results suggest that the genetic background of MMD in Asian populations is distinct from that in Western populations and that the low incidence of MMD in Western countries may be attributable to a lack of the founder *RNF213* mutation. (ii) Is unilateral involvement a subtype of MMD or a different disease?² We collected DNA samples from six patients with unilateral involvement and found a p.R4859K mutation in four of them (data not shown), suggesting that bilateral and unilateral MMD share a genetic background. (iii) Is pre-symptomatic diagnosis of MMD possible? In the present study, MMD never developed in the 15 mutation-negative family members in the 19 MMD families with the p.R4859K mutation (Table 3 and Supplementary Figure 1), suggesting the feasibility of presymptomatic diagnosis or exclusion by genetic testing.

How the mutant *RNF213* protein causes MMD remains to be elucidated. The expression of *RNF213* was more abundant in a subset of leukocytes than in the brain, suggesting that blood cells have a function in the etiology of MMD. This observation agrees with a previous report that MMD patients have systemic angiopathy.²⁰

Recent studies have suggested that the postnatal vasculature can form through vasculogenesis, a process by which endothelial progenitor cell are recruited from the splenic pool and differentiate into mature endothelial cells.²¹ Levels of endothelial progenitor cells in the peripheral blood are increased in MMD patients.²² *RNF213* may be expressed in splenic endothelial progenitor cells and mutant *RNF213* might dysregulate the function of the endothelial progenitor cells. Further research is necessary to elucidate the role of *RNF213* in the etiology of MMD.

CONFLICT OF INTEREST

The authors declare no conflict of interest.

ACKNOWLEDGEMENTS

We thank all of the patients and their families for participating in this study. We also thank Dr Hidetoshi Ikeda at the Department of Neurosurgery, Tohoku University School of Medicine and Drs Toshiaki Hayashi and Reizo Shirane at the Department of Neurosurgery, Miyagi Children's Hospital, Sendai, Japan for patient recruitment. We are grateful to Ms Kumi Kato for technical assistance. This study was supported by grants from the Ministry of Education, Culture, Sports, Science and Technology, Japan and by the Research Committee on Moyamoya Disease of the Ministry of Health, Labor and Welfare, Japan.

- 1 Suzuki, J. & Takaku, A. Cerebrovascular 'moyamoya' disease. Disease showing abnormal net-like vessels in base of brain. *Arch. Neurol.* **20**, 288–299 (1969).
- 2 Suzuki, J. *Moyamoya Disease* (Springer-Verlag: Berlin, 1983).
- 3 Oki, K., Hoshino, H. & Suzuki, N. In: *Moyamoya Disease Update*, (eds Cho B.K., Tominaga T.) 29–34 (Springer: New York, 2010).
- 4 Phi, J. H., Kim, S. K., Wang, K. C. & Cho, B. K. In: *Moyamoya Disease Update*, (eds Cho B.K., Tominaga T.) 82–86, (Springer: New York, 2010).
- 5 Yoshihara, T., Taguchi, A., Matsuyama, T., Shimizu, Y., Kikuchi-Taura, A., Soma, T. *et al.* Increase in circulating CD34-positive cells in patients with angiographic evidence of moyamoya-like vessels. *J. Cereb. Blood Flow Metab.* **28**, 1086–1089 (2008).
- 6 Achrol, A. S., Guzman, R., Lee, M. & Steinberg, G. K. Pathophysiology and genetic factors in moyamoya disease. *Neurosurg. Focus.* **26**, E4 (2009).
- 7 Scott, R. M. & Smith, E. R. Moyamoya disease and moyamoya syndrome. *N. Engl. J. Med.* **360**, 1226–1237 (2009).
- 8 Kure, S. In: *Moyamoya Disease Update* (eds Cho B.K., Tominaga T.) 41–45 (Springer: Tokyo, 2010).
- 9 Kuriyama, S., Kusaka, Y., Fujimura, M., Wakai, K., Tamakoshi, A., Hashimoto, S. *et al.* Prevalence and clinicoepidemiological features of moyamoya disease in Japan: findings from a nationwide epidemiological survey. *Stroke.* **39**, 42–47 (2008).
- 10 Sakurai, K., Horiuchi, Y., Ikeda, H., Ikezaki, K., Yoshimoto, T., Fukui, M. *et al.* A novel susceptibility locus for moyamoya disease on chromosome 8q23. *J. Hum. Genet.* **49**, 278–281 (2004).
- 11 Nanba, R., Kuroda, S., Tada, M., Ishikawa, T., Houkin, K. & Iwasaki, Y. Clinical features of familial moyamoya disease. *Childs. Nerv. Syst.* **22**, 258–262 (2006).
- 12 Ikeda, H., Sasaki, T., Yoshimoto, T., Fukui, M. & Arinami, T. Mapping of a familial moyamoya disease gene to chromosome 3p24.2–p26. *Am. J. Hum. Genet.* **64**, 533–537 (1999).
- 13 Inoue, T. K., Ikezaki, K., Sasazuki, T., Matsushima, T. & Fukui, M. Linkage analysis of moyamoya disease on chromosome 6. *J. Child. Neurol.* **15**, 179–182 (2000).
- 14 Yamauchi, T., Tada, M., Houkin, K., Tanaka, T., Nakamura, Y., Kuroda, S. *et al.* Linkage of familial moyamoya disease (spontaneous occlusion of the circle of Willis) to chromosome 17q25. *Stroke.* **31**, 930–935 (2000).
- 15 Wakai, K., Tamakoshi, A., Ikezaki, K., Fukui, M., Kawamura, T., Aoki, R. *et al.* Epidemiological features of moyamoya disease in Japan: findings from a nationwide survey. *Clin. Neurol. Neurosurg.* **99**(Suppl 2), S1–S5 (1997).
- 16 Mineharu, Y., Liu, W., Inoue, K., Matsuura, N., Inoue, S., Takenaka, K. *et al.* Autosomal dominant moyamoya disease maps to chromosome 17q25.3. *Neurology.* **70**, 2357–2363 (2008).
- 17 Liu, W., Hashikata, H., Inoue, K., Matsuura, N., Mineharu, Y., Kobayashi, H. *et al.* A rare Asian founder polymorphism of Raptor may explain the high prevalence of Moyamoya disease among East Asians and its low prevalence among Caucasians. *Environ. Health. Prev. Med.* **15**, 94–104 (2010).
- 18 Lupas, A. N. & Martin, J. AAA proteins. *Curr. Opin. Struct. Biol.* **12**, 746–753 (2002).
- 19 Ikezaki, K. In: *Moyamoya disease* (eds Ikezaki K., Loftus C. M.) 43–75 (Thieme: New York, 2001).
- 20 Ikeda, E. Systemic vascular changes in spontaneous occlusion of the circle of Willis. *Stroke.* **22**, 1358–1362 (1991).
- 21 Zampetaki, A., Kirton, J. P. & Xu, Q. Vascular repair by endothelial progenitor cells. *Cardiovasc. Res.* **78**, 413–421 (2008).
- 22 Rafat, N., Beck, G., Pena-Tapia, P. G., Schmiedek, P. & Vajkoczy, P. Increased levels of circulating endothelial progenitor cells in patients with Moyamoya disease. *Stroke.* **40**, 432–438 (2009).

Supplementary Information accompanies the paper on Journal of Human Genetics website (<http://www.nature.com/jhg>)

Supplementary Table 1. Genotyping of 384 SNPs within chromosome 17q25-ter in MMD patients.

No	SNP Name	Position	minor allele frequency	-logP (SNP)	-logP (Haplotype)***	gene
1	rs897595	74814739	0.23	0.54	0.60	
2	rs4790005	74820377	0.48	0.61	0.60	
3	rs4790007	74825355	0.49	0.56	0.56	
4	rs1869932	74830160	0.27	0.68	0.56	
5	rs897597	74833704	0.34	0.24		
6	rs4789887	74838408	0.35	0.16		
7	rs4790013	74846331	0.40	0.30		
8	rs8075376	74862253	0.16	0.18		
9	rs897600	74878104	0.38	1.59		
10	rs751848	74885572	0.35	0.24		
11	rs2034860	74891235	0.19	0.03		
12	rs9912528	74899145	0.18	0.21	0.98	
13	rs7225663	74902740	0.25	0.88	0.98	
14	rs897587	74907220	0.14	0.29		
15	rs2377405	74915689	0.27	0.23		
16	rs872016	74923774	0.19	**		
17	rs971626	74928535	0.48	0.71		
18	rs1007464	74932660	0.43	0.41		
19	rs4790037	74935348	0.42	1.07		
20	rs2137774	74947906	0.10	0.05		
21	rs884025	74965704	0.50	0.09		
22	rs871739	74973490	0.21	0.36		
23	rs7213580	74979416	n/a*	**		
24	rs4790051	74991920	n/a*	**		
25	rs211788	74995852	0.40	0.03		
26	rs9902874	75006934	n/a*	**		
27	rs11868921	75019989	n/a*	**		
28	rs12451031	75020299	n/a*	**		
29	rs7216806	75050112	0.46	0.66		
30	rs3935352	75257677	n/a*	**		
31	rs4074469	75269306	n/a*	**		
32	rs7208711	75286482	n/a*	**		
33	rs4555183	75294840	0.22	0.06		
34	rs6565697	75304120	n/a*	**		
35	rs8072313	75313636	n/a*	**		
36	rs8072274	75316196	0.46	0.06		
37	rs6565475	75316941	n/a*	**		
38	rs8074728	75319640	0.43	**		
39	rs11657217	75323934	0.21	0.80		
40	rs9900295	75329032	0.35	0.56		
41	rs8076446	75338179	0.28	0.79		
42	rs4243253	75342867	0.33	0.09	0.06	
43	rs4890049	75349284	0.08	**		
44	rs4889868	75354871	0.32	0.02	0.06	
45	rs6565539	75363556	0.06	0.11		
46	rs3829574	75368362	0.14	1.11		
47	rs3751956	75373079	0.21	0.59		
48	rs4889787	75375359	0.46	**		
49	rs8066940	75381216	0.19	0.83		
50	rs2587507	75404730	0.38	1.04		
51	rs7218526	75408455	0.21	1.58	1.82	
52	rs4889898	75412999	0.35	1.09	1.82	
53	rs1285251	75424418	0.32	**		
54	rs2289728	75426449	0.37	1.92	1.82	
55	rs3764374	75429891	0.18	0.32		
56	rs1622986	75438157	0.22	0.36		
57	rs1696756	75442568	0.31	1.48	1.48	
58	rs877874	75450416	0.26	1.62	1.48	
59	rs8078624	75459394	0.40	1.78	1.78	
60	rs1285264	75464091	0.40	0.16	1.78	
61	rs2362396	75469049	0.33	0.91	1.87	
62	rs4889796	75471233	0.28	1.87	1.87	
63	rs1285260	75477911	0.41	0.01		
64	rs8069143	75480095	0.26	0.34		
65	rs3843732	75486138	0.41	0.33		
66	rs4493093	75489976	0.29	0.15		
67	rs1285285	75496304	0.48	0.08		
68	rs1663183	75500655	0.16	0.11		
69	rs1663193	75505923	0.31	0.16		

70	rs4889802	75519064	0.15	0.16	
71	rs930551	75519744	0.05	0.69	
72	rs3169601	75524033	0.36	1.31	
73	rs1663196	75528635	0.21	0.59	
74	rs1285293	75539371	0.23	0.06	
75	rs7210391	75547666	0.13	0.75	
76	rs4889940	75553402	0.48	0.96	
77	rs1632673	75560331	0.08	0.32	
78	rs935200	75563386	0.39	**	
79	rs1115834	75564609	0.43	**	
80	rs4441315	75568048	0.49	0.93	
81	rs3934967	75578643	0.49	1.03	
82	rs11150827	75582679	0.28	0.06	0.01
83	rs7209428	75585536	0.22	0.31	0.01
84	rs4243249	75597441	0.28	1.02	
85	rs3764438	75626437	0.15	0.46	0.34
86	rs2289529	75636840	0.15	0.38	0.34
87	rs2289531	75638317	0.14	0.35	0.34
88	rs2289533	75638689	0.28	0.20	
89	rs9319623	75669201	0.42	0.81	
90	rs715041	75673027	0.26	2.17	2.64
91	rs1561811	75675223	0.26	0.73	2.64
92	rs4889954	75680189	0.25	0.00	2.64
93	rs2361701	75681212	0.30	1.54	2.64
94	rs2304854	75688157	0.49	0.42	2.64
95	rs2304851	75688355	0.21	0.85	2.64
96	rs1800307	75700466	0.22	2.23	2.64
97	rs2304836	75701441	0.23	**	
98	rs8132	75707948	0.15	0.64	
99	rs7211079	75722132	0.50	0.45	0.38
100	rs2289535	75726044	0.35	0.03	0.38
101	rs2241886	75728427	0.08	0.09	0.57
102	rs12601505	75739903	0.23	0.59	0.57
103	rs8065486	75752791	0.40	0.09	
104	rs12450100	75760213	0.08	0.09	
105	rs2289539	75766714	0.26	0.07	
106	rs4889990	75772590	0.22	0.23	
107	rs3829612	75775997	0.48	**	
108	rs8068433	75780051	0.40	0.77	
109	rs2018233	75784587	0.23	2.31	
110	rs755340	75784819	0.26	0.34	
111	rs3813063	75790449	0.39	1.47	
112	rs4889841	75808426	0.24	0.42	
113	rs6420489	75826801	0.25	0.10	
114	rs8078855	75839650	0.46	1.29	1.06
115	rs9915508	75845351	0.45	1.39	1.06
116	rs4889968	75851399	0.21	7.84	within RNF213
117	rs12449863	75857806	0.30	6.55	within RNF213
118	rs9902013	75861057	0.36	1.97	within RNF213
119	rs7219131	75867365	0.30	6.82	within RNF213
120	rs11869363	75881354	0.49	4.79	within RNF213
121	rs9905727	75887409	0.15	1.34	within RNF213
122	rs8066993	75894625	0.40	2.54	within RNF213
123	rs8081176	75898582	0.41	2.77	within RNF213
124	rs9674807	75900772	0.42	**	within RNF213
125	rs7501761	75904780	0.47	3.40	within RNF213
126	rs4890008	75920214	0.05	1.11	within RNF213
127	rs8074015	75920875	0.41	5.41	within RNF213
128	rs4890010	75930774	0.38	6.82	within RNF213
129	rs11150856	75937477	0.07	0.93	within RNF213
130	rs8067292	75948435	0.31	6.01	within RNF213
131	rs8070106	75959041	0.34	7.12	within RNF213
132	rs6565681	75963089	0.36	8.56	within RNF213
133	rs4889848	75969256	0.41	7.65	within RNF213
134	rs7224239	75969771	0.43	8.28	within RNF213
135	rs3185057	75978442	0.10	1.44	within RNF213
136	rs4603608	76003020	0.35	7.00	within RNF213
137	rs4077240	76012838	0.38	7.88	within FLJ35220
138	rs4491586	76022586	0.44	0.71	within FLJ35220
139	rs4074302	76034556	0.23	0.19	
140	rs8071962	76043498	0.41	**	
141	rs4890025	76047867	0.48	0.55	0.60

142	rs7503219	76054888	0.48	0.59	0.60
143	rs10931	76055642	0.05	0.41	
144	rs7213201	76071303	0.32	2.38	
145	rs4453556	76082006	0.33	1.32	1.30
146	rs4561525	76090663	0.38	2.92	1.30
147	rs9892081	76099079	0.28	1.42	1.30
148	rs3923514	76129805	0.43	0.41	0.41
149	rs7209040	76141889	0.30	1.21	0.41
150	rs901065	76214250	0.30	0.23	
151	rs8071015	76216967	0.24	1.01	
152	rs7212142	76238536	0.25	0.82	1.24
153	rs4889782	76255105	0.30	1.21	1.24
154	rs1485330	76255417	0.31	0.10	0.76
155	rs7217223	76260258	0.28	0.61	0.76
156	rs4255830	76263825	0.40	0.76	0.76
157	rs4889875	76266095	0.40	0.85	0.76
158	rs7208502	76284923	0.41	**	
159	rs7211818	76303498	0.28	0.91	0.98
160	rs6565478	76306599	0.36	0.98	0.98
161	rs4969230	76340856	0.47	0.37	
162	rs7208536	76364381	0.16	0.27	
163	rs4969266	76376141	0.48	0.01	
164	rs4969429	76379814	0.17	2.04	
165	rs734338	76396935	0.39	0.20	
166	rs2048753	76403883	0.34	0.11	0.82
167	rs2589133	76408071	0.40	0.01	0.82
168	rs2672901	76411261	0.31	0.82	0.82
169	rs746405	76426770	0.48	0.59	
170	rs7219745	76431503	0.30	0.13	
171	rs2589158	76433198	0.09	0.02	
172	rs3829572	76434807	0.47	0.63	0.55
173	rs3751945	76434924	0.47	0.63	0.55
174	rs2672893	76442458	0.36	0.15	0.55
175	rs2672890	76448802	0.39	0.62	0.08
176	rs2589118	76451148	0.47	0.08	0.08
177	rs6565484	76463451	0.38	0.92	1.56
178	rs11651707	76463905	0.34	1.19	1.56
179	rs7222366	76466229	0.38	1.04	1.56
180	rs2289762	76473705	0.38	1.04	1.56
181	rs2063788	76477893	0.42	1.95	1.56
182	rs868432	76492330	0.49	0.34	
183	rs2271602	76511083	0.49	0.16	0.13
184	rs4969227	76515193	0.15	0.04	0.13
185	rs4969311	76520955	0.26	0.02	0.13
186	rs1877926	76525636	0.50	0.09	0.13
187	rs1468032	76529982	0.47	0.13	0.13
188	rs2292639	76530550	0.47	0.13	
189	rs2271612	76534515	0.24	0.22	
190	rs7224748	76543615	0.40	0.01	
191	rs3751934	76553093	0.41	1.34	1.11
192	rs3751932	76554009	0.15	0.19	1.11
193	rs1062935	76554452	0.49	0.50	1.11
194	rs7502124	76559732	0.24	7.41	
195	rs1399571	76567065	0.23	0.10	0.20
196	rs7219486	76570569	0.24	0.28	0.20
197	rs884057	76576211	0.47	0.30	0.20
198	rs4969331	76581510	0.46	0.11	0.20
199	rs8081168	76585878	0.10	0.35	0.35
200	rs7219221	76593249	0.09	0.41	0.35
201	rs7225916	76607004	0.48	0.18	0.18
202	rs7502321	76608112	0.40	0.16	0.18
203	rs4969349	76620628	0.19	0.64	
204	rs4969355	76626942	n/a*	**	
205	rs12051877	76632362	0.39	1.10	
206	rs8067235	76639232	n/a*	**	
207	rs8079626	76641467	0.41	0.08	
208	rs11657991	76644343	n/a*	**	
209	rs4969367	76646610	0.18	0.97	
210	rs3934492	76648559	0.32	0.12	
211	rs9901648	76650303	n/a*	**	
212	rs4076037	76658879	0.50	0.61	
213	rs4969245	76671048	0.43	0.88	1.22

214	rs4969384	76680245	0.22	0.56	1.22
215	rs4969385	76683485	0.19	0.07	1.22
216	rs4075482	76689143	0.46	1.29	1.22
217	rs11664	76697457	0.43	1.10	1.22
218	rs4969394	76712771	0.22	0.03	
219	rs8073182	76719357	0.40	0.85	
220	rs9900420	76725990	0.15	0.50	
221	rs4969259	76733197	0.42	1.67	1.54
222	rs4969405	76737591	0.49	0.93	1.54
223	rs2174649	76741673	0.40	1.11	0.88
224	rs7209950	76747354	0.26	0.03	0.88
225	rs906189	76752666	0.40	0.95	0.88
226	rs4969415	76757647	0.24	1.64	
227	rs2659046	76760486	0.13	0.03	
228	rs7225354	76772657	0.22	0.31	
229	rs2292182	76778244	0.17	0.13	
230	rs906175	76788057	0.49	0.42	
231	rs2256881	76795370	0.16	0.61	
232	rs1048775	76816924	0.39	0.00	
233	rs6565548	76836926	0.23	**	
234	rs7224668	76850383	0.47	0.44	0.44
235	rs2292184	76859397	0.21	0.11	0.44
236	rs7212762	76869498	0.05	**	
237	rs11150780	76878755	0.14	0.16	0.44
238	rs6565549	76882829	0.38	0.02	
239	rs2048058	76893405	0.10	0.53	
240	rs6565550	76900586	0.15	0.50	
241	rs2864474	76916744	0.13	3.40	
242	rs7207673	76936167	0.33	0.59	
243	rs2279157	76938238	0.18	0.42	
244	rs9898002	76943559	0.07	0.15	
245	rs6565560	76948298	0.07	0.14	
246	rs899288	77001454	0.14	0.32	
247	rs7216513	77010284	0.13	0.17	
248	rs12601728	77015044	n/a*	**	
249	rs4969441	77021631	0.27	0.15	
250	rs6565570	77028031	0.28	2.96	2.96
251	rs899286	77031995	0.43	**	
252	rs6565571	77032855	0.30	2.85	2.96
253	rs14640	77047701	0.34	0.11	0.06
254	rs1984641	77057292	0.43	0.02	0.06
255	rs7406505	77073994	0.27	0.28	0.28
256	rs8079717	77083169	0.26	0.19	0.28
257	rs8182360	77086490	0.26	**	
258	rs7342974	77098594	0.08	0.07	0.28
259	rs7211870	77102086	0.10	0.13	0.28
260	rs2228698	77118981	0.30	0.70	
261	rs3924327	77128811	0.35	0.65	0.78
262	rs7207933	77131682	0.47	0.81	0.78
263	rs7405450	77150886	0.05	0.14	
264	rs7406859	77155280	0.04	0.33	
265	rs9894429	77207216	0.23	1.10	1.34
266	rs6565612	77213225	0.23	1.10	1.34
267	rs6565616	77222566	0.21	1.49	1.34
268	rs3830068	77233304	0.18	2.34	1.34
269	rs7502869	77241821	0.17	2.38	1.34
270	rs3088016	77250454	0.26	2.24	
271	rs6565624	77288155	0.19	2.13	
272	rs13912	77298298	0.31	0.73	
273	rs12449703	77303622	0.46	0.84	
274	rs9319620	77307788	0.43	0.49	
275	rs2070871	77398423	n/a*	**	
276	rs1057284	77420002	n/a*	**	
277	rs4433852	77449416	n/a*	**	
278	rs4539653	77479361	n/a*	**	
279	rs3744808	77484291	n/a*	**	
280	rs2293099	77491625	n/a*	**	
281	rs2102988	77505953	n/a*	**	
282	rs1879567	77508689	n/a*	**	
283	rs11539917	77534800	n/a*	**	
284	rs7405640	77542520	0.46	2.01	
285	rs8074498	77547833	0.32	**	

286	rs11077964	77559776	0.42	1.18	
287	rs9907483	77594188	0.35	0.39	
288	rs6502048	77598217	0.24	0.13	
289	rs4969484	77608150	0.41	**	
290	rs8068796	77615650	0.25	0.49	0.18
291	rs11655646	77624009	0.40	0.36	0.18
292	rs8066956	77627732	0.19	**	
293	rs4246444	77632241	0.39	0.15	
294	rs4502283	77638015	0.06	0.09	
295	rs6502057	77675349	0.09	0.52	0.52
296	rs7221544	77680626	0.09	0.52	0.52
297	rs8080423	77695568	0.09	0.52	0.52
298	rs7501461	77703095	0.08	0.72	0.52
299	rs7502078	77725168	0.09	0.52	0.52
300	rs8079572	77752141	0.06	0.30	0.52
301	rs4247357	77760278	0.09	0.52	0.52
302	rs4239020	77769930	0.06	0.33	
303	rs7503429	77784714	0.11	0.70	
304	rs9901910	77791296	0.21	0.61	
305	rs4789763	77882573	0.38	0.02	0.07
306	rs8079688	77883870	0.38	**	
307	rs12450996	77887398	0.49	2.31	0.07
308	rs8081117	77896844	0.07	1.30	
309	rs11654140	77925540	n/a*	**	
310	rs3935179	77935545	0.48	**	
311	rs11903	77943620	0.49	1.26	1.26
312	rs7503819	77944928	0.48	4.96	1.26
313	rs7211306	77960642	0.07	0.04	
314	rs1141463	77970979	0.36	1.00	0.89
315	rs7213057	77972228	0.35	0.70	0.89
316	rs4789773	77984973	0.09	0.24	
317	rs2306758	77995235	0.33	0.91	0.80
318	rs9303029	78002104	0.26	0.65	0.80
319	rs4789693	78015159	0.49	0.74	
320	rs2306752	78019924	0.14	0.57	
321	rs9909476	78033022	0.26	1.01	
322	rs1317685	78042986	0.38	1.75	
323	rs7221018	78049910	0.06	0.09	
324	rs8078417	78055224	0.32	0.56	
325	rs9911222	78066366	0.39	0.09	0.09
326	rs4789780	78072095	0.41	0.22	0.09
327	rs3803773	78079781	0.40	0.14	0.09
328	rs7502945	78088328	0.41	0.08	0.09
329	rs4789786	78097641	0.41	0.08	0.09
330	rs4789796	78114424	0.41	0.08	0.09
331	rs3736204	78123568	0.41	**	
332	rs4789799	78126368	0.19	0.48	0.09
333	rs1387545	78138144	0.43	0.17	
334	rs7215059	78143730	0.13	0.02	
335	rs3752821	78147635	0.14	0.13	
336	rs3794716	78152456	0.07	0.69	
337	rs4789704	78164349	0.24	0.21	
338	rs2306757	78167653	0.34	0.29	0.36
339	rs2306755	78181864	0.44	0.42	0.36
340	rs4789814	78186376	0.34	0.78	0.36
341	rs9303031	78195886	0.23	0.69	0.36
342	rs4789817	78201278	0.47	0.18	
343	rs2011631	78206350	0.18	0.32	
344	rs2279395	78210841	0.31	0.73	0.73
345	rs2279394	78211318	0.38	0.30	0.73
346	rs7211499	78218468	0.38	0.17	0.73
347	rs9912932	78220928	0.18	0.16	
348	rs4789708	78222126	0.28	0.64	
349	rs2247989	78229671	0.33	0.09	
350	rs11654159	78246238	0.03	1.42	
351	rs11869249	78261313	0.05	0.21	
352	rs2243523	78273738	0.41	1.86	
353	rs1046889	78278800	0.08	0.27	
354	rs2257084	78280764	0.44	0.70	
355	rs652265	78311676	0.43	0.49	0.68
356	rs629246	78350827	0.41	0.74	0.68
357	rs622789	78363101	0.41	0.72	0.68

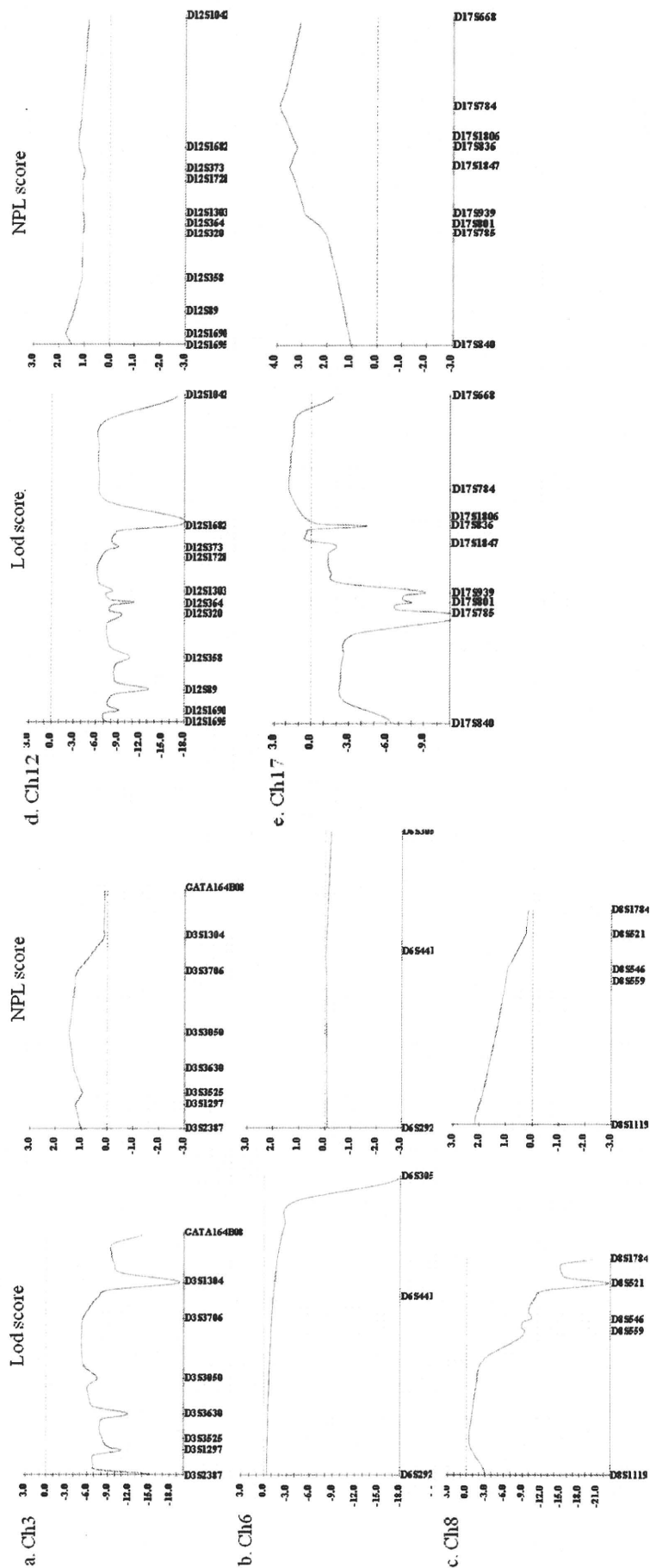
358	rs3744165	78383731	0.09	0.02	0.68
359	rs7225515	78389072	0.44	0.62	0.68
360	rs7219521	78395034	0.49	0.41	0.68
361	rs4986117	78402394	0.23	0.90	0.68
362	rs6502007	78412566	0.33	0.85	0.80
363	rs733342	78415369	0.23	1.05	0.80
364	rs8067926	78431877	0.32	2.08	
365	rs4986129	78446843	0.03	7.28	
366	rs1551625	78470842	0.23	1.22	
367	rs1078334	78477536	0.43	2.46	
368	rs3785512	78479817	0.14	0.47	2.38
369	rs898095	78483927	0.36	3.10	2.38
370	rs3785521	78489058	0.27	2.55	2.38
371	rs1001865	78508277	0.23	0.71	2.38
372	rs9303016	78517996	0.17	1.13	
373	rs7209936	78519504	0.47	1.21	
374	rs1551628	78528901	0.33	6.03	
375	rs6502033	78541807	0.49	0.73	
376	rs12601298	78552287	0.27	0.04	
377	rs9893868	78564747	0.38	**	
378	rs7222550	78578613	0.23	0.79	
379	rs4986140	78583049	0.46	1.56	
380	rs9890099	78587132	0.43	0.51	
381	rs967825	78593728	0.48	0.18	1.22
382	rs7224733	78598059	0.23	1.22	1.22
383	rs6502040	78605474	0.31	0.44	1.22
384	rs3935099	78609338	0.32	1.30	

In the case of $-\log P > 4.96$ ($P < 1.10 \times 10^{-5}$), P -values remain significant at the below 0.05 after 10,000 permutations.

* Not available.

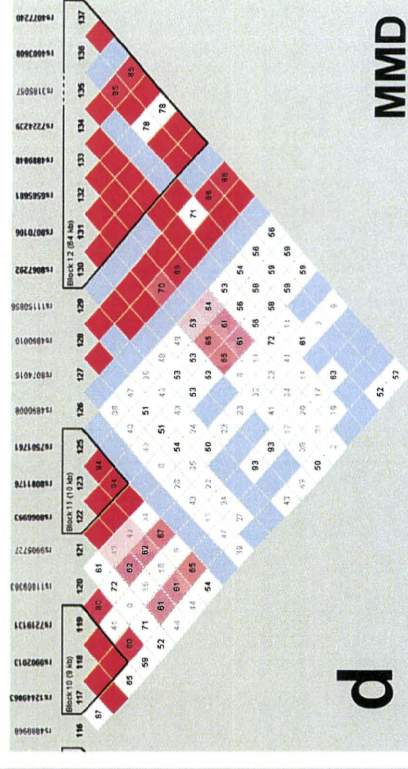
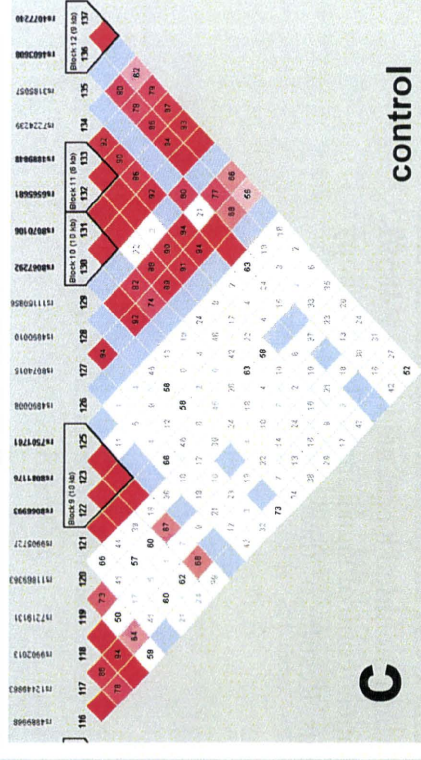
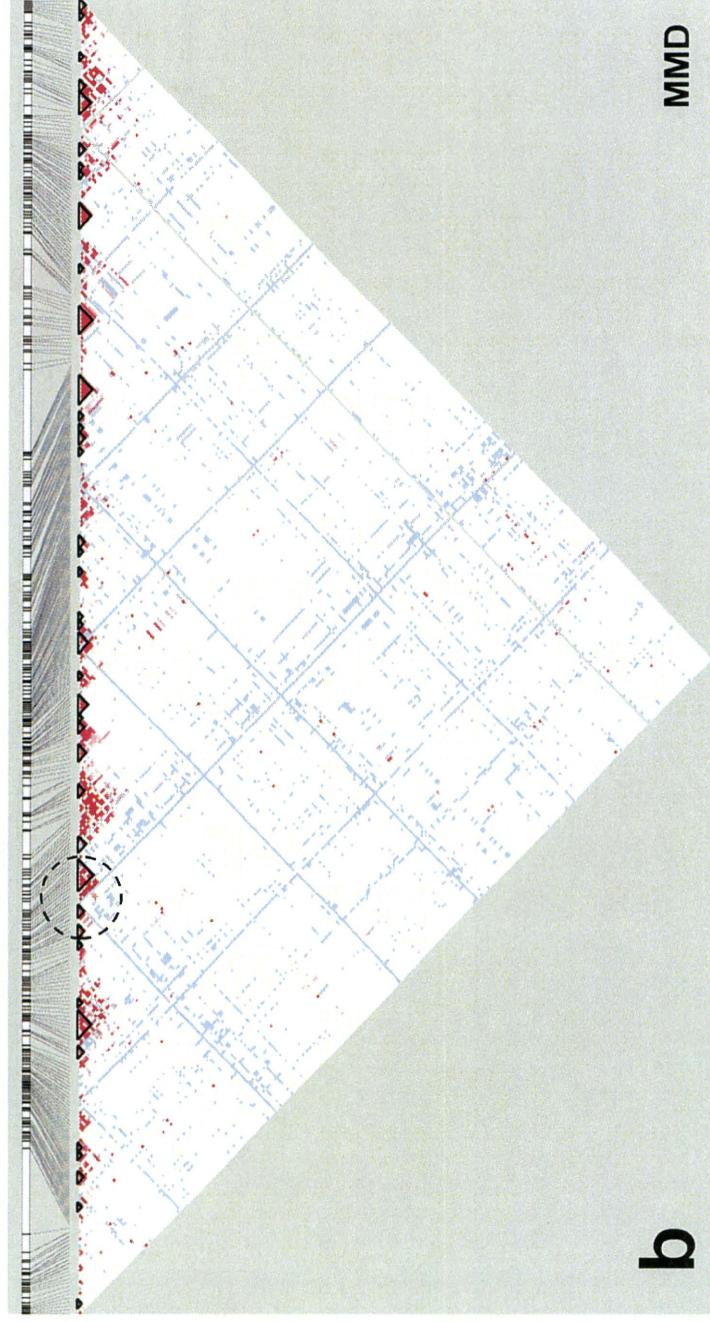
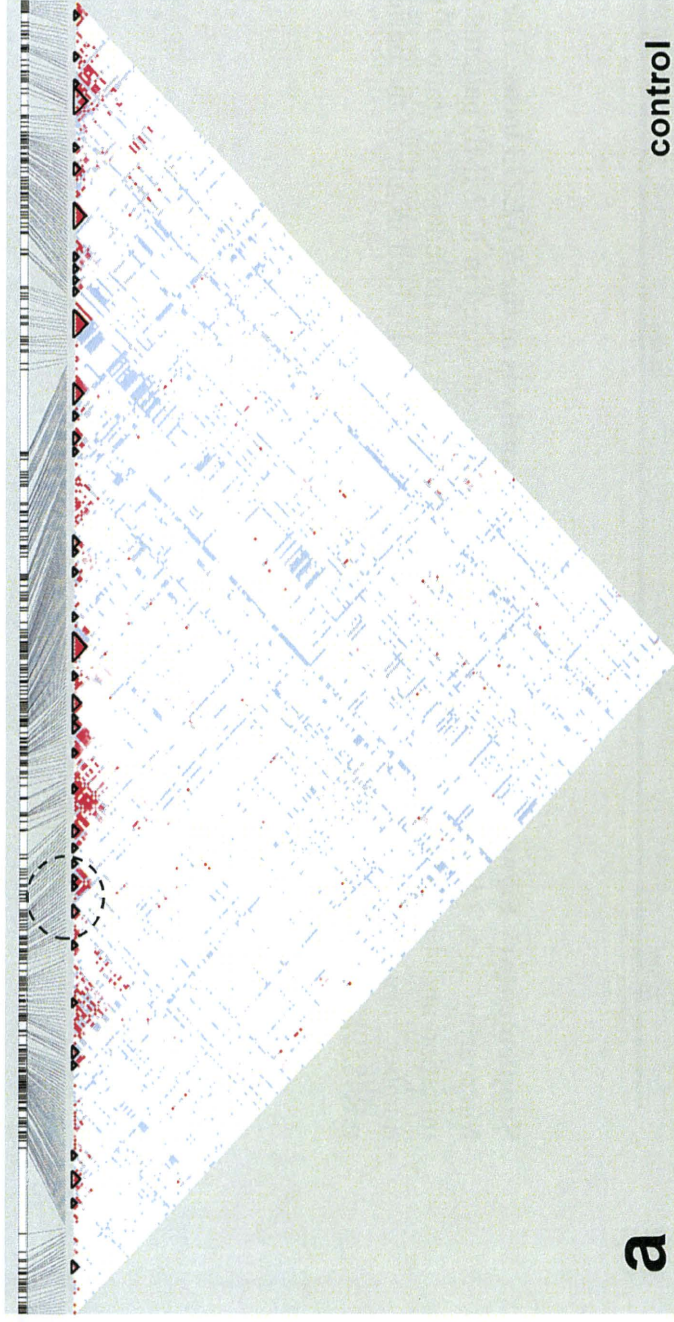
** Genotyping was unsuccessful because the base call rate was less than 95%.

*** The $-\log P$ (Haplotype) shows P -value of the major haplotype.



Supplementary Figure 2. Linkage analysis of 20 Japanese MMD families

Twenty MMD families were studied by genotyping of the microsatellite markers, which were previously used for identification of five candidate chromosome loci for MMD genes. Highest linkage score was observed at the microsatellite marker D17S784 on chromosome 17q25, the Lod score 2.4 and the NPL score 3.8, which was suggestive but not definitive.



Supplementary Figure 3. Structure of the linkage disequilibrium (LD) block in Japanese control subjects (a) and patients with MMD (b). Dotted circles in panels a and b indicate the regions of the higher magnification images in panels c and d, respectively.